Chin. Phys. B Vol. 22, No. 3 (2013) 030209

Multisymplectic implicit and explicit methods for Klein–Gordon–Schrödinger equations*

Cai Jia-Xiang(蔡加祥)†, Yang Bin(杨 斌), and Liang Hua(梁 华)

School of Mathematical Science, Huaiyin Normal University, Huai'an 223300, China

(Received 12 July 2012; revised manuscript received 5 September 2012)

We propose multisymplectic implicit and explicit Fourier pseudospectral methods for the Klein–Gordon–Schrödinger equations. We prove that the implicit method satisfies the charge conservation law exactly. Both methods provide accurate solutions in long-time computations and simulate the soliton collision well. The numerical results show the abilities of the two methods in preserving the charge, energy, and momentum conservation laws.

Keywords: Klein–Gordon–Schrödinger equations, multisymplectic method, Fourier pseudospectral method, conservation law

PACS: 02.60.Cb, 02.70.Bf, 45.10.Na, 02.70.Hm **DOI:** 10.1088/1674-1056/22/3/030209

1. Introduction

The Klein–Gordon–Schrödinger (KGS) equations are

$$k\psi_t + \frac{1}{2}\psi_{xx} + \psi\phi = 0, \quad \phi_{tt} - \phi_{xx} + \phi - |\psi|^2 = 0, \tag{1}$$

where $\psi(x,t)$ represents a complex scalar nucleon field, $\phi(x,t)$ a real scalar meson field, and $k = \sqrt{-1}$ describes a system of conserved scalar nucleons interacting with neutral scalar mesons through the Yukawa interaction. With the initial and periodic conditions

$$\begin{aligned} \psi(x,0) &= \psi_0(x), \quad \phi(x,0) = \phi_0(x), \quad \phi_t(x,0) = \phi_1(x), \\ \psi(a,t) &= \psi(b,t), \quad \phi(a,t) = \phi(b,t), \end{aligned} \tag{2}$$

the KGS equations possess the following conservation laws.

- The charge conservation law

$$\mathscr{Q}(t) = \int_a^b |\psi(x,t)|^2\,\mathrm{d}x = \int_a^b |\psi(x,0)|^2\,\mathrm{d}x = \mathscr{Q}(0). \tag{3}$$

- The energy conservation law

$$\begin{aligned} \mathscr{E}(t) &= \int_a^b (\phi(x,t)^2 + \phi_t(x,t)^2 + \phi_x(x,t)^2 + |\psi_x(x,t)|^2 \\ &\quad - 2\phi(x,t)|\psi(x,t)|^2)\,\mathrm{d}x = \mathscr{E}(0). \end{aligned} \tag{4}$$

- The momentum conservation law

$$\begin{aligned} \mathscr{M}(t) &= \int_a^b \Im(\overline{\psi}(x,t)\psi_x(x,t) - \phi_t(x,t)\phi_x(x,t))\,\mathrm{d}x \\ &= \mathscr{M}(0). \end{aligned} \tag{5}$$

A massive number of numerical and theoretical analyses of the KGS equations have been performed over the years. More recently, studying with numerical approximations has become a hot topic, and now some reliable efficient numerical methods[1–5] have been proposed to solve the KGS equations. Since the concept of a multisymplectic integrator was first proposed,[6,7] much attention has been paid to it.[8–23] Kong *et al.*[21] first noted that the KGS equations have a natural multisymplectic structure and then derived the multisymplectic Preissman scheme. In Ref. [22], Kong *et al.* developed a linearly implicit symplectic Fourier pseudospectral scheme. Hong *et al.*[23] proposed a series of fully explicit multisymplectic schemes for the KGS equations by concatenating suitable symplectic Runge–Kutta-type methods and symplectic Runge–Kutta–Nyström-type methods. The aim of this work is to construct new implicit and explicit methods for the KGS equations (1). Then we will examine the numerical performances of the proposed methods.

The rest of this paper is organized as follows. In Section 2, we construct multisymplectic methods for the KGS equations. We prove that the implicit method satisfies the charge conservation law exactly. Numerical simulations of the propagation and collision solutions are presented in Section 3, and the conclusions are given in Section 4.

2. Multisymplectic methods for KGS equations

By setting $\psi(x,t) = p(x,t) + kq(x,t)$, where $p(x,t)$ and $q(x,t)$ are real-valued functions, the KGS equations (1) can be written as

$$\begin{aligned} &p_t + \frac{1}{2}q_{xx} + \phi q = 0, \\ &-q_t + \frac{1}{2}p_{xx} + \phi p = 0, \\ &\phi_{tt} - \phi_{xx} + \phi - (p^2 + q^2) = 0. \end{aligned} \tag{6}$$

*Project supported by the Young Scientists Fund of the National Natural Science Foundation of China (Grant No. 11201169) and the Natural Science Foundation of the Jiangsu Higher Education Institutions of China (Grant No. 10KJB110001).

†Corresponding author. E-mail: thomasjeer@sohu.com

By introducing new variables $p_x = f$, $q_x = r$, $\phi_t = v$, and $\phi_x = w$, equation (6) can be reformulated in the following first-order form:

$$\begin{aligned}
&-q_t + \frac{1}{2} f_x = -\phi p, \quad -\frac{1}{2} p_x = -\frac{1}{2} f, \\
&p_t + \frac{1}{2} r_x = -\phi q, \quad -\frac{1}{2} q_x = -\frac{1}{2} r, \\
&-\frac{1}{2} v_t + \frac{1}{2} w_x = \frac{1}{2} \phi - \frac{1}{2}(p^2 + q^2), \\
&\frac{1}{2} \phi_t = \frac{1}{2} v, \quad -\frac{1}{2} \phi_x = -\frac{1}{2} w,
\end{aligned} \tag{7}$$

or the general form of the multisymplectic Hamiltonian system[21]

$$\boldsymbol{M} \boldsymbol{z}_t + \boldsymbol{K} \boldsymbol{z}_x = \nabla_{\boldsymbol{z}} S(\boldsymbol{z}), \tag{8}$$

where $\boldsymbol{z} = (p, q, f, r, \phi, v, w)^{\mathrm{T}}$, $\boldsymbol{M}$ and $\boldsymbol{K}$ are two skew-symmetric matrices

$$\boldsymbol{M} = \begin{pmatrix}
0 & -1 & 0 & 0 & 0 & 0 & 0 \\
1 & 0 & 0 & 0 & 0 & 0 & 0 \\
0 & 0 & 0 & 0 & 0 & 0 & 0 \\
0 & 0 & 0 & 0 & 0 & 0 & 0 \\
0 & 0 & 0 & 0 & 0 & -\frac{1}{2} & 0 \\
0 & 0 & 0 & 0 & \frac{1}{2} & 0 & 0 \\
0 & 0 & 0 & 0 & 0 & 0 & 0
\end{pmatrix},$$

$$\boldsymbol{K} = \begin{pmatrix}
0 & 0 & \frac{1}{2} & 0 & 0 & 0 & 0 \\
0 & 0 & 0 & \frac{1}{2} & 0 & 0 & 0 \\
-\frac{1}{2} & 0 & 0 & 0 & 0 & 0 & 0 \\
0 & -\frac{1}{2} & 0 & 0 & 0 & 0 & 0 \\
0 & 0 & 0 & 0 & 0 & 0 & \frac{1}{2} \\
0 & 0 & 0 & 0 & 0 & 0 & 0 \\
0 & 0 & 0 & 0 & -\frac{1}{2} & 0 & 0
\end{pmatrix},$$

and the Hamiltonian function $S(\boldsymbol{z}) = -\frac{1}{2}\phi(p^2+q^2) + \frac{1}{4}(\phi^2 + v^2 - w^2 - f^2 - r^2)$. System (8) admits the multisymplectic conservation law

$$\partial_t \omega + \partial_x \kappa = 0, \tag{9}$$

where $\omega = \mathrm{d}\boldsymbol{z} \wedge \boldsymbol{M} \mathrm{d}\boldsymbol{z} = -2\mathrm{d}p \wedge \mathrm{d}q - \mathrm{d}\phi \wedge \mathrm{d}v$ and $\kappa = \mathrm{d}\boldsymbol{z} \wedge \boldsymbol{K} \mathrm{d}\boldsymbol{z} = \mathrm{d}p \wedge \mathrm{d}f + \mathrm{d}q \wedge \mathrm{d}r + \mathrm{d}\phi \wedge \mathrm{d}w$.

In order to establish numerical methods, we set $x_j = jh$, $j = 0, 1, 2, \ldots, N$ and $t_n = n\tau$, $n = 1, 2, \ldots$, where $h = (b-a)/N$ and τ are spatial and temporal step sizes, respectively. We also define the difference and average operators as

$$\delta_t^{\pm} z_i^n = \pm(z_i^{n\pm1} - z_i^n)/\tau, \quad \mathrm{A}_t z_i^n = (z_i^n + z_i^{n+1})/2.$$

As we know, the first-order differential operator ∂_x yields the Fourier spectral differentiation matrix $\boldsymbol{D}_1$. Here, $\boldsymbol{D}_1$ is an $N \times N$ skew-symmetric matrix with elements

$$(D_1)_{i,j} = \begin{cases} \frac{1}{2}\mu(-1)^{i+j}\cot(\mu\frac{x_i - x_j}{2}), & i \neq j, \\ 0, & i = j, \end{cases}$$

where $i, j = 1, 2, \ldots, N$, and $\mu = 2\pi/(b-a)$. For more details, one can consult Ref. [10] and the references therein. Inspired by the technique used in Ref. [10], we discrete Eq. (7) with the Fourier pseudospectral method in the space domain, and then we obtain a semi-discrete system

$$\begin{aligned}
&\frac{\mathrm{d}q_i}{\mathrm{d}t} + \frac{1}{2}(\boldsymbol{D}_1 \boldsymbol{f})_i = -\phi_i p_i, \quad (\boldsymbol{D}_1 \boldsymbol{p})_i = f_i, \\
&\frac{\mathrm{d}p_i}{\mathrm{d}t} + \frac{1}{2}(\boldsymbol{D}_1 \boldsymbol{r})_i = -\phi_i q_i, \quad (\boldsymbol{D}_1 \boldsymbol{q})_i = r_i, \\
&-\frac{\mathrm{d}v_i}{\mathrm{d}t} + (\boldsymbol{D}_1 \boldsymbol{w})_i = \phi_i - (p_i^2 + q_i^2), \\
&\frac{\mathrm{d}\phi_i}{\mathrm{d}t} = v_i, \quad (\boldsymbol{D}_1 \boldsymbol{\Phi})_i = w_i,
\end{aligned} \tag{10}$$

where $\boldsymbol{f} = (f_0, f_1, \ldots, f_{N-1})^{\mathrm{T}}$, $\boldsymbol{p} = (p_0, p_1, \ldots, p_{N-1})^{\mathrm{T}}$, $\boldsymbol{r} = (r_0, r_1, \ldots, r_{N-1})^{\mathrm{T}}$, $\boldsymbol{q} = (q_0, q_1, \ldots, q_{N-1})^{\mathrm{T}}$, $\boldsymbol{w} = (w_0, w_1, \ldots, w_{N-1})^{\mathrm{T}}$, and $\boldsymbol{\Phi} = (\phi_0, \phi_1, \ldots, \phi_{N-1})^{\mathrm{T}}$. Equation (10) can be rewritten in the compact form

$$\boldsymbol{M}\frac{\mathrm{d}z_i}{\mathrm{d}t} + \boldsymbol{K}\sum_{j=0}^{N-1}(D_1)_{i,j} z_j = \nabla_{\boldsymbol{z}} S(z_i). \tag{11}$$

Theorem 1 The Fourier pseudospectral semi-discrete (11) has N semi-discretization multisymplectic conservation laws[10]

$$\frac{\mathrm{d}}{\mathrm{d}t}\omega_i + \sum_{j=0}^{N-1}(D_1)_{i,j}\kappa_{i,j} = 0, \quad i = 0, 1, 2, \ldots, N-1, \tag{12}$$

where $\omega_i = \frac{1}{2}(\mathrm{d}z_i \wedge \boldsymbol{M}\,\mathrm{d}z_i)$, and $\kappa_{i,j} = \mathrm{d}z_i \wedge \boldsymbol{K}\,\mathrm{d}z_j$.

Since matrix $\boldsymbol{D}_1$ is skew-symmetric and $\kappa_{i,j} = \kappa_{j,i}$, summing Eq. (12) over the spatial index i gives the total symplectic conservation law $\frac{\mathrm{d}}{\mathrm{d}t}\sum_{i=0}^{N-1}\omega_i = 0$. Therefore, we should choose a symplectic integration in the time direction for Eq. (11) in order to preserve the global symplecticity.

The implicit multisymplectic scheme Applying the symplectic midpoint rule with respect to time derivatives in the compact form (11) yields

$$\boldsymbol{M}\delta_t^+ z_i^n + \boldsymbol{K}\sum_{j=0}^{N-1}(D_1)_{i,j} z_j^{n+\frac{1}{2}} = \nabla_{\boldsymbol{z}} S(z_i^{n+\frac{1}{2}}). \tag{13}$$

Theorem 2 The Fourier pseudospectral full-discretization (13) has N full-discrete multisymplectic conservation laws

$$\delta_t^+ \omega_i^n + \sum_{j=0}^{N-1}(D_1)_{i,j}\kappa_{i,j}^{n+\frac{1}{2}} = 0, \quad i = 0, 1, 2, \ldots, N-1, \tag{14}$$

where $\omega_i^n = \mathrm{d}z_i^n \wedge \boldsymbol{M}\,\mathrm{d}z_i^n$, and $\kappa_{i,j}^n = \mathrm{d}z_i^{n+\frac{1}{2}} \wedge \boldsymbol{K} dz_j^{n+\frac{1}{2}}$.

Taking the wedge product of the variational equation associated with Eq. (11) with $\mathrm{d}z_i^{n+1/2}$ and calculating carefully, we can prove the theorem. Expanding Eq. (13) reads

$$\begin{aligned}
&-\delta_t^+ q_i^n + \frac{1}{2}(\boldsymbol{D}_1 \boldsymbol{f}^{n+\frac{1}{2}})_i = -\phi_i^{n+\frac{1}{2}} p_i^{n+\frac{1}{2}}, \\
&(\boldsymbol{D}_1 \boldsymbol{p}^{n+\frac{1}{2}})_i = f_i^{n+\frac{1}{2}}, \\
&\delta_t^+ p_i^n + \frac{1}{2}(\boldsymbol{D}_1 \boldsymbol{r}^{n+\frac{1}{2}})_i = -\phi_i^{n+\frac{1}{2}} q_i^{n+\frac{1}{2}}, \quad (\boldsymbol{D}_1 \boldsymbol{q}^{n+\frac{1}{2}})_i = r_i^{n+\frac{1}{2}},
\end{aligned}$$

$$-\delta_t^+ v_i^n + (\boldsymbol{D}_1 \boldsymbol{w}^{n+\frac{1}{2}})_i = \phi_i^{n+\frac{1}{2}} - [(p_i^{n+\frac{1}{2}})^2 + (q_i^{n+\frac{1}{2}})^2],$$
$$\delta_t^+ \phi_i^n = v_i^{n+\frac{1}{2}}, \quad (\boldsymbol{D}_1 \boldsymbol{\Phi}^{n+\frac{1}{2}})_i = w_i^{n+\frac{1}{2}}. \tag{15}$$

Eliminating the auxiliary variables gives an implicit multisymplectic scheme

$$\delta_t^+ q_i^n - \frac{1}{2} \mathrm{A}_t (\boldsymbol{D}_1^2 \boldsymbol{p}^n)_i - (\mathrm{A}_t \phi_i^n)(\mathrm{A}_t p_i^n) = 0, \tag{16a}$$
$$\delta_t^+ p_i^n + \frac{1}{2} \mathrm{A}_t (\boldsymbol{D}_1^2 \boldsymbol{q}^n)_i + (\mathrm{A}_t \phi_i^n)(\mathrm{A}_t q_i^n) = 0, \tag{16b}$$
$$\delta_t^+ \delta_t^+ \phi_i^n - \mathrm{A}_t^2 (\boldsymbol{D}_1^2 \boldsymbol{\Phi}^n)_i + \mathrm{A}_t^2 \phi_i^n - \mathrm{A}_t [(\mathrm{A}_t p_i^n)^2 + (\mathrm{A}_t q_i^n)^2] = 0. \tag{16c}$$

Now, we turn to investigate the discrete analogue of the discrete charge conservation law. We define the inner product and the 2-norm of vectors as

$$(\boldsymbol{u}, \boldsymbol{v}) = h \sum_{i=0}^{N-1} u_i \bar{v}_i, \quad \| \boldsymbol{u} \| = \sqrt{(\boldsymbol{u}, \boldsymbol{u})} = \sqrt{h \sum_{i=0}^{N-1} |u_i|^2}.$$

Theorem 3 The multisymplectic scheme (16) satisfies the charge conservation law exactly, namely,

$$\mathscr{Q}^{n+1} = \| \Psi^{n+1} \|^2 = \mathscr{Q}^n = \cdots = \mathscr{Q}^0. \tag{17}$$

Proof Multiplying Eqs. (16a) and (16b) by $2\mathrm{A}_t q_i^n$ and $2\mathrm{A}_t p_i^n$, respectively, and then summing the results, we have

$$\frac{1}{\tau}(| \psi_i^{n+1} |^2 - | \psi_i^n |^2) - (\boldsymbol{D}_1^2 \boldsymbol{p}^{n+\frac{1}{2}})_i q_i^{n+\frac{1}{2}} + (\boldsymbol{D}_1^2 \boldsymbol{q}^{n+\frac{1}{2}})_i p_i^{n+\frac{1}{2}} = 0. \tag{18}$$

Taking the discrete inner product of Eq. (18) yields

$$\frac{1}{\tau}(\| \Psi^{n+1} \|^2 - \| \Psi^n \|^2) - (\boldsymbol{D}_1^2 \boldsymbol{p}^{n+\frac{1}{2}}, \boldsymbol{q}^{n+\frac{1}{2}}) + (\boldsymbol{D}_1^2 \boldsymbol{q}^{n+\frac{1}{2}}, \boldsymbol{p}^{n+\frac{1}{2}}) = 0. \tag{19}$$

Further, we have $-(\boldsymbol{D}_1^2 \boldsymbol{p}^{n+\frac{1}{2}}, \boldsymbol{q}^{n+\frac{1}{2}}) + (\boldsymbol{D}_1^2 \boldsymbol{q}^{n+\frac{1}{2}}, \boldsymbol{p}^{n+\frac{1}{2}}) = 0$ since matrix $\boldsymbol{D}_1^2$ is symmetrical. Thus, equation (17) is proved.

The explicit multisymplectic scheme Although the scheme (16) satisfies the discrete charge conservation law, the weakness of the scheme is that it is implicit. This results in a huge expense in numerically solving the systems of the nonlinear equations at each time step. Therefore, efficient and stable explicit schemes are of value in many cases. Applying the symplectic Euler rule to the compact form (11) with respect to time yields

$$\boldsymbol{M}_+ \delta_t^+ z_i^n + \boldsymbol{M}_- \delta_t^- z_i^n + \boldsymbol{K} \sum_{j=0}^{N-1} (D_1)_{i,j} z_j^n = \boldsymbol{\nabla}_{\boldsymbol{z}} S(z_i^n), \tag{20}$$

where $\boldsymbol{M}_+$ and $\boldsymbol{M}_-$ are splitting matrices of the symplectic structure matrix $\boldsymbol{M}$, i.e., $\boldsymbol{M} = \boldsymbol{M}_+ + \boldsymbol{M}_-$, $\boldsymbol{M}_+^{\mathrm{T}} = -\boldsymbol{M}_-$.

Theorem 4 The Fourier pseudospectral discretization (20) has N full-discrete multisymplectic conservation laws

$$\delta_t^+ \omega_i^n + \sum_{j=0}^{N-1} (D_1)_{i,j} \kappa_{i,j}^n = 0, \quad i = 0, 1, 2, \ldots, N-1, \tag{21}$$

where $\omega_i^n = \mathrm{d}z_i^{n-1} \wedge \boldsymbol{M}_+ \mathrm{d}z_i^n$, and $\kappa_{i,j}^n = \mathrm{d}z_i^n \wedge \boldsymbol{K} \mathrm{d}z_j^n$.

Proof The variational equation associated with Eq. (20) is

$$\boldsymbol{M}_+ \delta_t^+ \mathrm{d}z_i^n + \boldsymbol{M}_- \delta_t^- \mathrm{d}z_i^n + \boldsymbol{K} \sum_{j=0}^{N-1} (D_1)_{i,j} \mathrm{d}z_j^n = S_{zz}(z_i^n) \mathrm{d}z_i^n. \tag{22}$$

Taking the wedge product of Eq. (22) with $\mathrm{d}z_i^n$, and then noting $\mathrm{d}z_i^n \wedge S_{zz}(z_i^n) \mathrm{d}z_i^n = 0$ and

$$\begin{aligned} & \mathrm{d}z_i^n \wedge \boldsymbol{M}_+ \delta_t^+ \mathrm{d}z_i^n + \mathrm{d}z_i^n \wedge \boldsymbol{M}_- \delta_t^- \mathrm{d}z_i^n \\ = {} & \mathrm{d}z_i^n \wedge \boldsymbol{M}_+ \delta_t^+ \mathrm{d}z_i^n + \delta_t^- \mathrm{d}z_i^n \wedge \boldsymbol{M}_+ \mathrm{d}z_i^n \\ = {} & \delta_t^+ (\mathrm{d}z_i^{n-1} \wedge \boldsymbol{M}_+ \mathrm{d}z_i^n), \end{aligned}$$

we obtain N full-discrete multisymplectic conservation laws (14).

Obviously, the splitting matrices are not unique. Different splitting matrices may lead to different schemes. Here, we take $\boldsymbol{M}_+$ as the upper triangle matrix and $\boldsymbol{M}_-$ as the lower triangle matrix. With this choice, expanding Eq. (20) yields

$$\delta_t^+ q_i^n + \frac{1}{2}(D_1 \boldsymbol{f}^n)_i = -\phi_i^n p_i^n, \quad (\boldsymbol{D}_1 \boldsymbol{p}^n)_i = f_i^n,$$
$$\delta_t^- p_i^n + \frac{1}{2}(\boldsymbol{D}_1 \boldsymbol{r}^n)_i = -\phi_i^n q_i^n, \quad (\boldsymbol{D}_1 \boldsymbol{q}^n)_i = r_i^n,$$
$$-\delta_t^+ v_i^n + (\boldsymbol{D}_1 \boldsymbol{w}^n)_i = \phi_i^n - [(p_i^n)^2 + (q_i^n)^2],$$
$$\delta_t^- \phi_i^n = v_i^n, \quad (\boldsymbol{D}_1 \boldsymbol{\Phi}^n)_i = w_i^n. \tag{23}$$

Eliminating the auxiliary variables gives an explicit scheme

$$-\delta_t^+ q_i^n + \frac{1}{2}(\boldsymbol{D}_1^2 \boldsymbol{p}^n)_i + \phi_i^n p_i^n = 0,$$
$$\delta_t^- p_i^n + \frac{1}{2}(\boldsymbol{D}_1^2 \boldsymbol{q}^n)_i + \phi_i^n q_i^n = 0,$$
$$\delta_t^+ \delta_t^- \phi_i^n - (\boldsymbol{D}_1^2 \boldsymbol{\Phi}^n)_i + \phi_i^n - [(p_i^n)^2 + (p_i^n)^2] = 0. \tag{24}$$

3. Numerical simulations

In this section, we will conduct some numerical experiments to test the performances of the multisymplectic implicit scheme (16) and the multisymplectic explicit scheme (24). The performances of the two schemes are exhibited in the following aspects: the accuracies of the single soliton solution and the numerical performances in preserving the conservative quantities, including charge $\mathscr{Q}$, energy $\mathscr{E}$, and momentum $\mathscr{M}$. The accuracy of the migration of a soliton at $t_n = n\tau$ is measured by

$$\| L(\psi) \|_\infty = \max_{0 \le i \le N-1} | \psi(x_i, n\tau) - \psi_i^n |,$$
$$\| L(\psi) \|_2 = \left(h \sum_{i=0}^{N-1} | \psi(x_i, n\tau) - \psi_i^n |^2 \right)^{1/2}.$$

Similarly, we can define $\| L(\phi) \|_\infty$ and $\| L(\phi) \|_2$. The discrete charge, energy, and momentum quantities at $t_n = n\tau$ are calculated by

$$\begin{aligned}
\mathscr{Q}^n &= h \sum_{i=0}^{N-1} |\psi_i^n|^2, \\
\mathscr{E}^n &= h \sum_{i=0}^{N-1} [(\phi_i^n)^2 + (\delta_t^- \phi_i^n)^2 + (\boldsymbol{D}_1 \boldsymbol{\Phi}^n)_i^2 + |(\boldsymbol{D}_1 \boldsymbol{\Psi}^n)_i|^2 \\
&\quad - 2\phi_i^n |\psi_i^n|^2], \\
\mathscr{M}^n &= h \sum_{i=0}^{N-1} \Im(\delta_t^- \overline{\psi_i^n} (\boldsymbol{D}_1 \boldsymbol{\Psi}^n)_i - \delta_t^- \phi_i^n (\boldsymbol{D}_1 \boldsymbol{\Psi}^n)_i).
\end{aligned}$$

The errors in charge, energy, and momentum are scaled by $|\mathscr{Q}^n - \mathscr{Q}^0|$, $|\mathscr{E}^n - \mathscr{E}^0|$, and $|\mathscr{M}^n - \mathscr{M}^0|$, respectively.

Example 1 (single soliton) The KGS equations (1) admit analytic solitary wave solutions

$$\begin{aligned}
\psi(x,t,\nu,x_0) &= \frac{3\sqrt{2}}{4\sqrt{1-\nu^2}} \operatorname{sech}^2 \left(\frac{1}{2\sqrt{1-\nu^2}} (x - \nu t - x_0) \right) \\
&\quad \times \exp \left[\mathrm{i} \left(\nu x + \frac{1 - \nu^2 + \nu^4}{2(1-\nu^2)} t \right) \right], \\
\phi(x,t,\nu,x_0) &= \frac{3}{4(1-\nu^2)} \\
&\quad \times \operatorname{sech}^2 \left(\frac{1}{2\sqrt{1-\nu^2}} (x - \nu t - x_0) \right), \qquad (25)
\end{aligned}$$

where ν is the propagating velocity of the wave, and x_0 is the initial phase. In this test, we solve the initial problem $\psi_0(x) = \psi(x,t,0.1,0)$, $\phi_0(x) = \phi(x,t,0.1,0)$, and $\phi_1(x) = \phi_t(x,t,0.1,0)|_{t=0}$ over region $-10 \le x \le 10$ up to $T = 80$. The implicit and explicit schemes are implemented with $N = 200$, $\tau = 0.01$ and $N = 200$, $\tau = 0.001$, respectively. The error norms in $|\psi|$ and ϕ of the two schemes are shown in Figs. 1 and 2. From Fig. 2, we find that the errors in solutions $|\psi|$ and ϕ oscillate near zero in the scale of 10^{-4} and do not exhibit any growth throughout the computations. Therefore, the implicit method (16) can provide accurate solutions in long-time computations. From Fig. 3, we can see that the errors obtained by the explicit method (24) also oscillate near zero, but they increase as time evolves. However, the errors are still small at $T = 80$. Figure 3 displays the errors in charge, energy, and momentum of the two methods. From Fig. 3(a), we find that the implicit scheme satisfies the charge conservation law exactly since the errors in charge are within the roundoff error of the machine. The energy and momentum are conserved very well because the errors are in the scale of 10^{-8}. From Fig. 3(b), it is clear that the explicit scheme preserves the three conservative quantities well.

Next, we compare the performance of our implicit method with that of the methods in the literature. We consider the problem with $\nu = 0.3$, $x_0 = -20$, $-40 \le x \le 40$ and implement all methods with various temporal and spatial step sizes. Table 1 lists the numerical errors for all methods at $T = 1$. The charge errors are also listed in the table. From the table, we find that the proposed implicit method provides the second-best numerical solutions, ψ and ϕ, while it preserves the charge quantity better than the others.

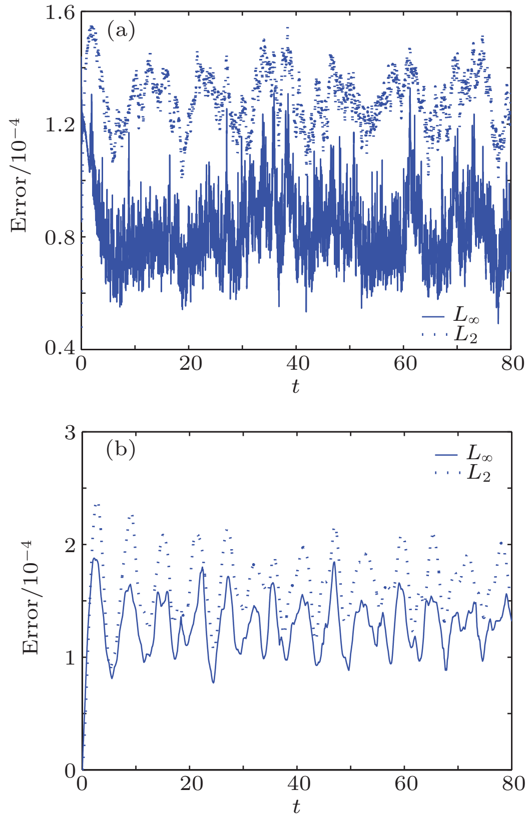

Fig. 1. (color online) The errors in the solutions of (a) $|\psi|$ and (b) ϕ obtained by the implicit scheme (16).

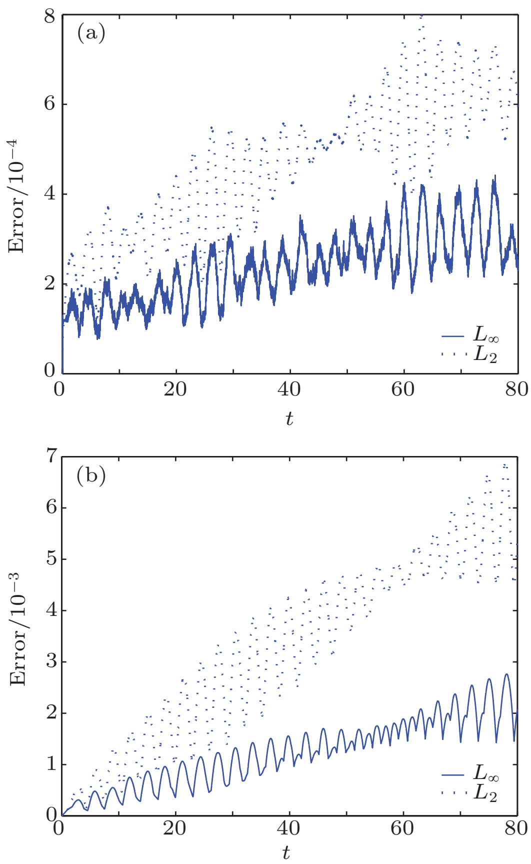

Fig. 2. (color online) The errors in the solutions of (a) $|\psi|$ and (b) ϕ obtained by the explicit scheme (24).

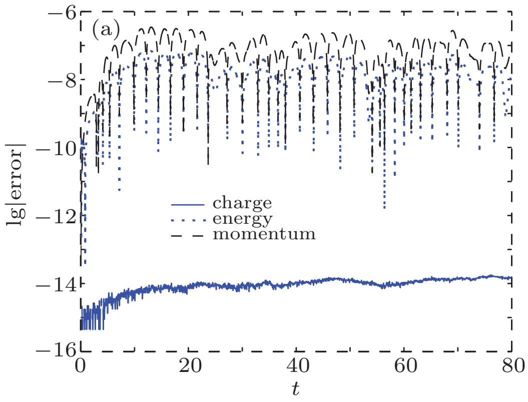

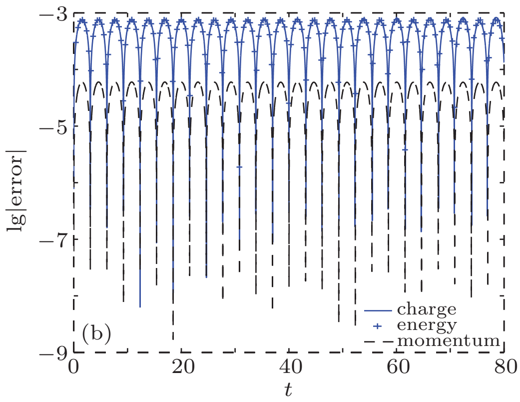

Fig. 3. (color online) The errors in the invariants for (a) the implicit scheme and (b) the explicit scheme.

Table 1. Comparison among several methods in numerical error and conserved quantities.

τ/h	Method	$\parallel L(\phi)\parallel_\infty$	$\parallel L(\psi)\parallel_\infty$	$\lvert Q^n - Q^0\rvert$
0.1/0.2	scheme (16)	3.0277×10^{-4}	2.8025×10^{-4}	4.4409×10^{-16}
	Ref. [1]	1.2586×10^{-3}	2.0780×10^{-3}	5.7731×10^{-15}
	Ref. [21]	3.4042×10^{-3}	5.0322×10^{-3}	4.4409×10^{-15}
	Ref. [22]	1.0009×10^{-4}	1.6686×10^{-4}	1.4210×10^{-14}
0.05/0.1	scheme (16)	7.9757×10^{-5}	7.4593×10^{-5}	4.4409×10^{-16}
	Ref. [1]	3.3251×10^{-4}	5.3927×10^{-4}	1.1102×10^{-14}
	Ref. [21]	9.5158×10^{-5}	1.3354×10^{-3}	7.5495×10^{-15}
	Ref. [22]	2.9594×10^{-5}	4.1465×10^{-5}	2.6201×10^{-14}

Example 2 (soliton collision) In the following simulations, we study the head-on collisions of two solitary waves. The initial conditions are chosen as

$$\begin{aligned}\psi_0 &= \psi(x,0,v_1,x_1)+\psi(x,0,v_2,x_2),\\ \phi_0 &= \phi(x,0,v_1,x_1)+\phi(x,0,v_2,x_2),\\ \phi_1 &= \phi(x,t,v_1,x_1)_t|_{t=0}+\phi(x,t,v_2,x_2)|_{t=0}.\end{aligned}\tag{26}$$

We solve the problem with $N=150$ and $\tau=0.001$ in region $-30\le x\le 30$ up to $T=80$, and investigate the collision of the symmetric solitons. We take $v_1=0.2$, $x_1=-10$ and $v_2=-0.2$, $x_2=10$. The solitons are symmetric if they are symmetrically distributed around the origin. Figure 4 displays the evolutions of the shapes of $|\psi|$ and ϕ. Figure 5 shows the errors in charge, energy, and momentum of the two methods. From Fig. 5(a), we find that the implicit scheme preserves the charge exactly and conserves the energy well. From the two graphs in Fig. 5, we can see that the errors in the momentum of the two schemes are all about 10^{-13}. As we know, the two schemes do not preserve the momentum exactly. The reason for the errors to be 10^{-13} is that the momentum is zero for the symmetric soliton collision case.

Next, we discuss the non-symmetric soliton collision. We choose $v_1=0.4$, $x_1=-20$ and $v_2=-0.2$, $x_2=15$. The simulations of the soliton collision are illustrated in Fig. 6. It is clear that the soliton with a large amplitude becomes larger and the one with a small amplitude becomes smaller after the collision. The errors in charge, energy, and momentum of the two schemes are represented in Fig. 7.

Example 3 (plane wave solution) We study the evolution of a plane wave as time evolves. The KGS equations admit the analytic plane wave solution

$$\begin{cases}\psi(x,t)=\exp[\mathrm{i}(7x+48t)],\\ \phi(x,t)=1,\end{cases}\qquad 0\le x\le 4\pi.\tag{27}$$

Obviously, the modular of the wave is always equal to 1. Thus, we call it a plane wave because the modular of the wave forms a plane parallel to the x–t plane. Here, we take $\psi_0(x)=\exp(7\mathrm{i}x)$, $\phi_0(x)=1$ and $\phi_1(x)=48\mathrm{i}\exp[\mathrm{i}(7x+48t)]$ as the initial conditions. We conduct the simulations with $N=40$ and $\tau=0.001$ up to $T=100$. Figure 8 shows the variations in the maximum errors in $|\psi|$ and ϕ against time. We can see that the errors in ϕ obtained by the two schemes are almost the same, while the errors in $|\psi|$ obtained by the implicit scheme are much smaller than those of the explicit scheme. Figure 9 exhibits the residuals of the conservative quantities, charge, energy, and momentum, of the two schemes. It is clear that the implicit scheme preserves the three invariants much better than the explicit one.

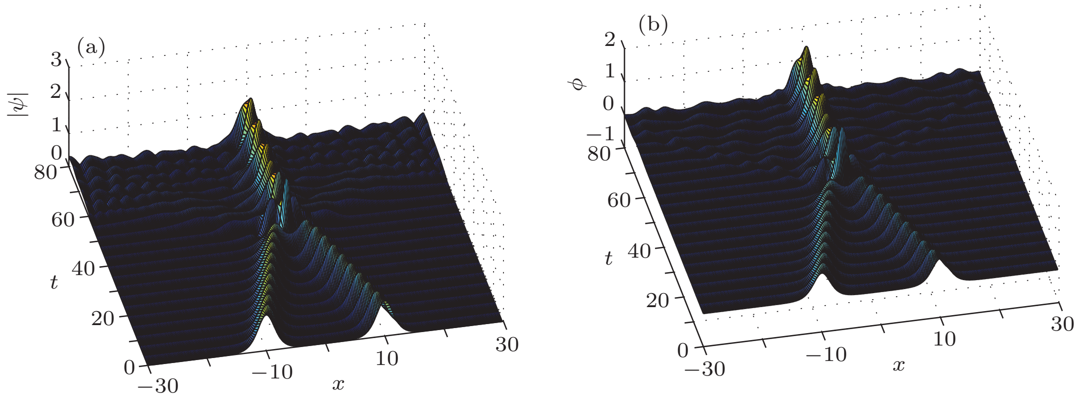

Fig. 4. (color online) The collision of symmetric solitons: (a) $|\psi|$, (b) ϕ.

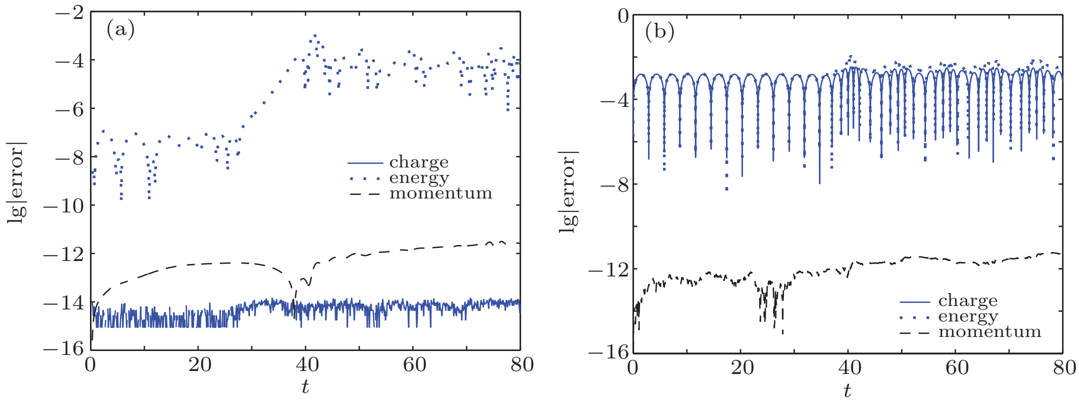

Fig. 5. (color online) The errors in the invariants of the symmetric soliton collision in (a) the implicit scheme, and (b) the explicit scheme.

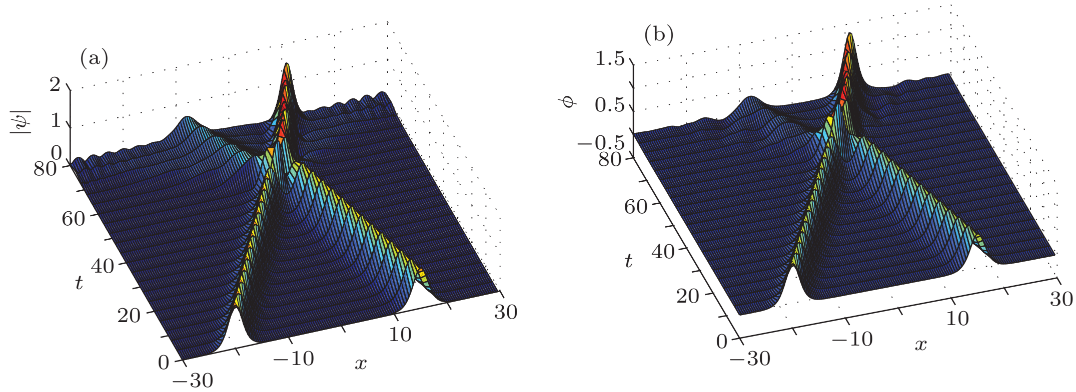

Fig. 6. (color online) The collision of non-symmetric solitons: (a) $|\psi|$, (b) ϕ.

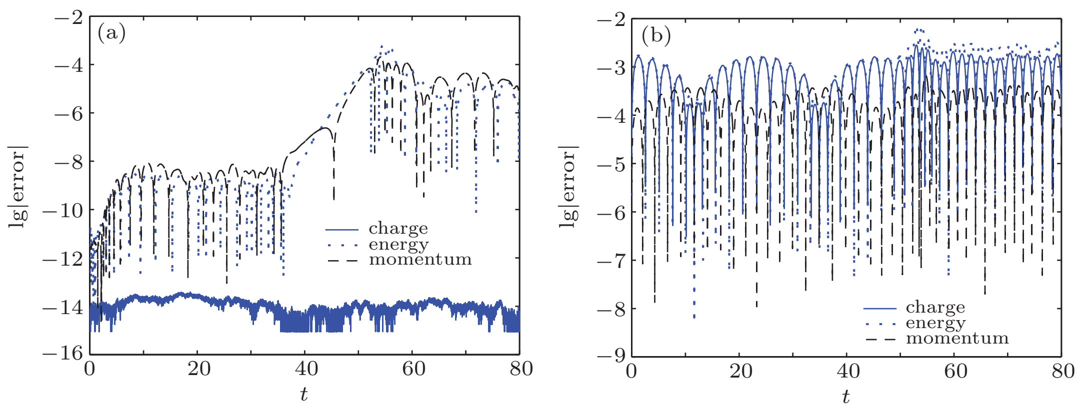

Fig. 7. (color online) The errors in the invariants of the collision of non-symmetric solitons in (a) the implicit scheme, and (b) the explicit scheme.

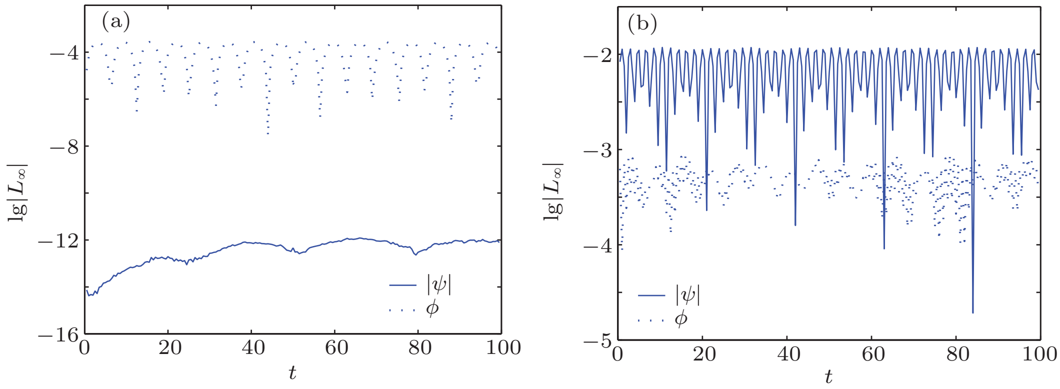

Fig. 8. (color online) The maximum errors in $|\psi|$ and ϕ for (a) the implicit scheme, and (b) the explicit scheme.

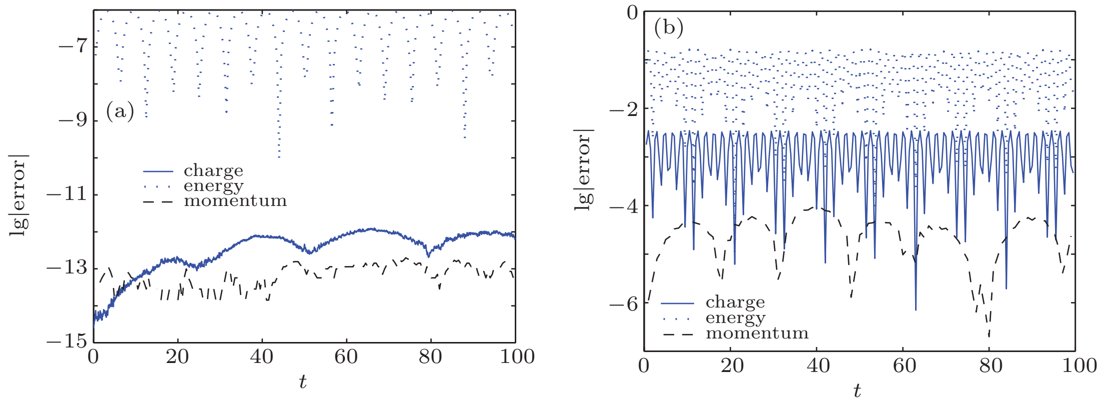

Fig. 9. (color online) The errors in charge, energy, and momentum for (a) the implicit scheme, and (b) the explicit scheme.

4. Conclusion

Applying the Fourier pseudospectral method to space derivatives and the symplectic rule to time derivatives in the multisymplectic form (8) of the KGS equations, we construct implicit and explicit multisymplectic schemes. The implicit scheme satisfies the charge conservation law exactly. In long-time computations, the two methods both provide satisfactory solutions for a single soliton and simulate the collision of solitons well. In all the numerical experiments, both methods preserve the invariants well. Although the implicit scheme conserves the invariants better than the explicit one, while the latter is easier to be implemented than the former.

References

[1] Zhang L 2005 *Appl. Math. Comput.* **163** 343
[2] Xanthopoulos P and Zouraris G E 2008 *Discrete Contin. Dyn. Syst. Ser. B* **10** 239
[3] Wang S and Zhang L 2008 *Appl. Math. Comput.* **203** 799
[4] Xiang X 1988 *J. Comput. Appl. Math.* **21** 161
[5] Bao W and Yang L 2007 *J. Comput. Phys.* **225** 1863
[6] Marsden J E, Patrick G P and Shkoller S 1998 *Comm. Math. Phys.* **199** 351
[7] Bridges T J and Reich S 2001 *Phys. Lett. A* **284** 184
[8] Reich S 2000 *J. Comput. Phys.* **157** 473
[9] Ascher U M and McLachlan R I 2004 *Appl. Numer. Math.* **48** 255
[10] Chen J B and Qin M Z 2001 *Electron. Trans. Numer. Anal.* **12** 193
[11] Hu W P and Deng Z C 2008 *Chin. Phys. B* **17** 3923
[12] Wang Y S and Li S T 2010 *Inter. J. Comput. Math.* **87** 775
[13] Lv Z Q, Xue M and Wang Y S 2011 *Chin. Phys. Lett.* **28** 060205
[14] Cai J X and Miao J 2012 *Chin. Phys. Lett.* **29** 030201
[15] Qian X, Song S H, Gao E and Li W B 2012 *Chin. Phys. B* **21** 070206
[16] Zhang R P, Yu X J and Feng T 2012 *Chin. Phys. B* **21** 030202
[17] Wang H and Li B 2011 *Chin. Phys. B* **20** 040203
[18] Wang J 2009 *J. Phys. A: Math. Theor.* **42** 085205
[19] Hong J L and Kong L H 2010 *Commun. Comput. Phys.* **7** 613
[20] Sun Y and Tse P S P 2011 *J. Comput. Phys.* **230** 2076
[21] Kong L H, Liu R and Xu Z 2006 *Appl. Math. Comput.* **181** 342
[22] Kong L H, Zhang J J, Cao Y, Duan Y and Huang H 2010 *Comput. Phys. Commun.* **181** 1369
[23] Hong J L, Jiang S S and Li C 2009 *J. Comput. Phys.* **228** 3517